IMPLEMENTATION OF HIGH-SPEED VECTOR CONTROL SRM FOR ELECTRIC VEHICLE

[1]Ashok Pedapudi, [2]V V Satyavathi Yedida, [3]Srinivas Mekala
[1,2,3]Assistant Professor, [1,2,3,4]Department of Mechanical Engineering, Rishi MS Institute of Engineering and Technlogy for Women, Kukatpally, Hyderabad.

ABSTRACT
The high speed motor works well to accomplish motor reduction in an electric vehicle (EV). Due to the rotor's straightforward and durable construction, Switched Reluctance Motors (SRM) is appropriate for high speed drives. The tremor and acoustic noise are substantial, though, which is a drawback. Additionally, the complexity of the unipolar current excitation contributes to the challenge of designing a torque controller. For SRM, the vector control has been suggested as a solution to these issues. The SRM, however, has not been subject to vector control in the high speed zone. This study clarifies the drive conditions for applying vector control to the SRM in the high speed zone, such as switching frequency and bus voltage. It is shown by the experiment that the proposed SRM can be driven by the vector control in the high speed region and can realize the high output power and low vibration.
Keywords: Switched reluctance motor, high speed drive, Vector control

1. INTRODUCTION

Gas emissions must now be drastically reduced due to their impact on the ozone layer due to a growing outcry from environmental activists and government legislation [1]. Internal Combustion Engines (ICE) power conventional transportation systems (vehicles), which cause the environment to be harmed by the burning of gas and fuel into hydrocarbon oxides. While research has focused on renewable energy sources, it has also advanced and evolved hybrid electric vehicles (HEVs), which employ both internal combustion engines and electric motors to move their wheels [2-4]. Additionally, fully electric vehicles (EVs) have been available and operating since that time [5]. These automobiles are propelled by one or more electric motors [6]. Researchers are now exploring use of renewable energy including solar, wind and tidal waves for sustainable mobility [7-10].

An electric vehicle consists of three major subsystems; the energy source subsystem, the auxiliary subsystem and the electronic propulsion subsystem [3,11,12]. The electronic propulsion subsystem comprises an electronic controller, the power converter, the mechanical transmission and
the electric motor. In this work, a review of different motors available as propulsion for electric vehicle is presented (Fig. 1).

The development of electrical drives dates back to the 18th century when Faraday demonstrated the principle of electromagnetic induction [14]. Following a proposal of Faraday's law, electric motors were invented and that bred the two major classes of motors: Alternating Current and Direct Current motors.

Typically, an electric motor consists of a rotor, stator, windings, air gap and commutators/ converters. Depending on a different arrangement of these components different types of electric motors are constructed [15]. Those electric motors that do not require brushes for commutation or energy conversion are called brushless permanent magnet motors [16]. Furthermore, motors can be categorized according to the shape of their back Electromotive-Force (Back-EMF). Their shape can either be sinusoidal or trapezoidal. Based on their construction and energy interchange principles, they can be Permanent Magnet AC Synchronous Motors (PMSM) or Brushless DC motors (BLDC) [17].

For an electric motor to be successfully deployed as the drive for EVs, it should be highly efficient, it should have great power density and should be cost-effective [11]. Furthermore, motor drives in EVs, unlike industrial motors and conveyors, require; frequent start/stops, high rates of acceleration/deceleration, high torque at low speed, low torque at high-speed and wide speed ranges. However, the specification of the motor depends on its application. This application includes systems for home usage, regular vehicle and heavy-duty vehicles. Furthermore, the performance of motors depends mainly on vehicle duty cycle, thermal characteristics and the cooling mechanism implemented [11]. The classification of various motors used in traction is shown in Figure A brief literature review on the motors used for traction in EV/HEVs is presented below. In this work, a literature review of both AC and DC motors is presented on the basis of the features mentioned earlier.

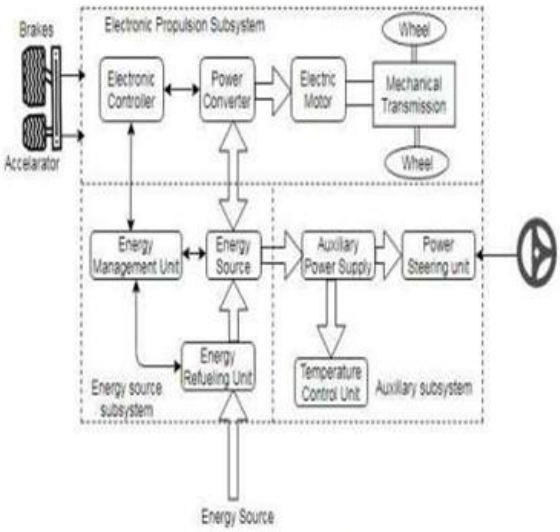

Fig. 1. Block diagram of an electric vehicle [13]

2. RELATED WORK

Switched reluctance motor is having higher speed than the stepper motor, lacking the use of expensive permanent magnets. It contains desirable qualities of an AC induction motor, a DC motor and a brushless motor. The SRM is also an economical alternative to other synchronous and induction machines for higher torque and higher speed applications (Li et al. 2019). For the past few decades, air pollution is a major concern for the environment. Most of the air pollution is due to the consumption of fuels in automobiles. For the reduction in air pollution level in terms of environment, electric vehicles are credible (Suresh et al. 2020; Karthik et al. 2020; Subasri et al. 2020; Sheela et al. 2020). Most of the electric vehicles are manufactured with the switched reluctance motor (SRM). SRMs are used in electric vehicles due to their tailor-made characteristics (Aiso, Takahashi, and Akatsu 2019).

The conventional SRMs show all these characteristics, but have some drawbacks too, i.e. such as torque ripples, noise and magnetic saturation (Qianfan, Shumei, and Xinjia 2007). All these things are responsible for their unsatisfactory efficiency in the operations. For enhancing their efficiencies, several types of topologies are invented by the researchers with unique and distinctive features despite having a few disadvantages.

In, an alternative method of increasing torque profile has been proposed in which successful optimised design has been carried out and discussed the reason which sets barrier in its popularity. Double rotor topology is a unique topology suggested in Qianfan, Shumei, and Xinjia (2007)for improvement in efficiency. The novel dual-mode SRM (Miller 1989) has the characteristics of both a synchronous machine and a conventional SRM. Another effective way to uplift the torque by increasing the number of rotor poles is presented in Sun et al. (2019), which, in turn, results in a bulkier design and higher cost of machine.

In Li, Ravi, and Aliprantis (2016) the rotor poles of SRM have been modified in order to reduce magnetic saturation and increased torque. In this paper, the stator poles of the conventional SRM are modified and a novel

topology is proposed in order to increase its torque profile and reduction in the mass of the material. The proposed topology consists of a slotted stator tooth at a certain depth by removing some portion of the core material. The winding of the proposed SRM motor is similar to the conventional model.

This will serve the purpose, i.e. for providing a new path to the magnetic flux lines flowing across the core, for reducing core material and make it cost effective and for reducing the weight of the motor. After optimising the new topology, the flux linkage and torque have been calculated and analysed using the finite element method (FEM). The comparison is made between the conventional model and proposed model to justify the characteristics of the proposed model are superior (Yang 2015; Kiyota et al. 2019; Desai et al. 2010; Zhu et al. 2017).

Controllability Of Vector Control For SRM

A. Principle and current controller of vector control

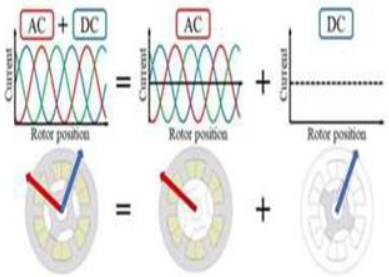

Fig.2. Vector Control of SRM

The vector control of the SRM is depicted in Figure. This is a three-phase sinusoidal DC offset current that arouses the subject. A revolving magnetic field is generated by the current component of the stator. A magnetic flux vector is generated by the direct current component, which is determined by the location of the rotor. Magnetic stream that runs through the rotor field is represented by the rotor field vector. It is possible to generate torque by interacting with the rotating magnetic field of the stator and the rotor's magnetic flux.

The vector control system of the SRM generates torque by the use of mathematical calculations. [9]

[10]. In the equivalent SRM's voltage equation, the zero-phase volume is represented by the d-q axis. This equation defines the self-inductance of a wire coil in terms of zero-phase voltage and a DC component of the voltage along the d-axis, a zero-phase volume, and a zero-phase voltage component.

The DC component can be utilised to derive the zero-phase component of the excitation current by subtracting it from the total current (3). It may be calculated by utilising the second term of the inductance matrix (2), which is represented by the formula:The inertia of the virtual rotor is denoted by the letter I in the symbol. Figure shows how zero-phase current generates virtual rotor flows as a function of time. In order to compute the SRM torque, the following equation is used: Or, to put it another way, there are two points of view on this issue. (5) There are more than double the number of people who have zero queries as there were previously. If I had to guess, I would say that when we compare zero-phase currents to rotational torque and flux currents, we find that they are extremely close in terms of magnitude and frequency.

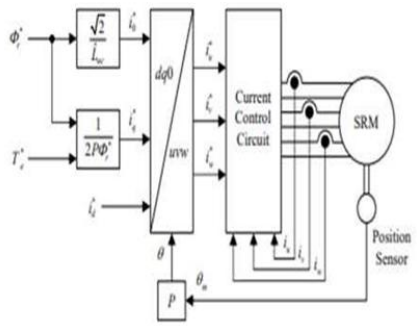

Fig.3. Vector Control System for SRM Drive

In depth investigation of the existing controller is performed by [13]. Currently available vector control controllers are depicted in Figure. depicts the current PI controller, the disconnecting controller, and the feed forward controller in operation. The voltage commands from those controllers can be processed by a carrier-based PWM inverter. The PI controller is responsible for maintaining control of the current flowing through each axis and phase of the circuit. The following is the syntax used for the function transfer:

It has a time constant of one tenth of a second, which is extremely fast. The managed SRM can be recognized as the rotating reference framework's RL circuits as a result of decoupling and forward control mechanisms. For the optimal single order current response, make sure that c equals the controlled machine's time constant (Ldc/R), as shown in the diagram. The Kc gain is established by the present response speed of a system under consideration. One of the goals of this research is to duplicate and test an existingcontroller.

PROPOSED SRM

Table I contains the specs of the two SRMs depicted in Figure, one with a 12-pin configuration and eight poles and the other with a 30-pin design and twenty poles. The 12-pin configuration with eight poles SRM is the smaller of the two SRMs. When designing the 20-pole, 30-slot SRM, it was important to consider that it would have the same electric angular frequency and electrical characteristics as the 8-pole, 12-slot SRM in order to demonstrate controllability at high rotational speeds.

$$f_m = N_m \times \frac{P}{60}$$

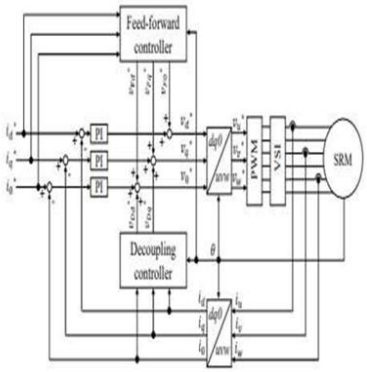

Fig.4. Current Controller for Vector Control

B. Controllability of high speed drive

The switching frequency and bus voltage, as well as the required power and rotational speed of 20000rpm, are determined by these parameters. The simulation analyses the current and torque waveforms at a speed of 20,000

rotations per minute and a reference torque of 16.2 Nm. Figure depicts the current and torque waveforms associated with the switching frequency. The harmonic distortion and current wave ratio are affected by the frequency at which the switch is made. When it comes to harmonic distortions, the phrases current ripple ratio (CRR) and effective value of the harmonic current order are used to characterise the phenomenon (I1).

The current amplitudes at their maximum, minimum, and average values are given by the variables imax, imin, and iave, which stand for maximum, minimum, and average, respectively. A q-axis as well as zero-phase THD and current rippling ratios are shown in Table II for the switching frequency, which is also shown in Figure. As shown in Figure and Table, the switching frequency decreases with increasing switching frequency, and the THD and current ripple rate decrease with increasing switching frequency. Due to increased iron loss produced by harmonic fluxes on the high-speed motor, it is important to keep the total harmonic distortion (THD) to a minimum.

3. PROPOSED SYSTEM AND SIMULATION RESULTS

It is possible for an electric motor to rotate at a maximum rotational frequency of 60 P f N (1), where fm is the maximum electric frequency, Nm is the maximum rotational frequency, and P is the number of poles. In accordance with the specifications, the Model A can operate at a maximum electrical frequency of 6.67 kHz (1). A twenty-poled model with a maximum rotational speed of 20,000 revolutions per minute, the same as Model A, is also on the market. Both SRMs have the same outside diameter, stack length, and air gap length, as well as the same interior diameter. Their auto-inductance distributions, in addition, exhibit almost the same variance as the distributions depicted in Figure. In order to estimate the SRM torque, use the following calculation:

$$T = \frac{P}{2}\frac{\partial L}{\partial \theta} i^2$$

In the equation P L T I, the letters P, L, and I stand for torque output, inductance, electric angle, and current, in that order (2). As the number of poles rises, the torque increases in a linear fashion

(2). The Model B has a torque that is 2.5 times more than the Model A. Providing the same amount of torque as Model A should necessitate 0.63 times the current consumption of Model B. Figure depicts the current characteristics of the situation. 'torque' is an abbreviation for torque. Model B torque is 2.5 times stronger than Model A torque when no magnetic saturation area is fitted with the same current as the Model A torque (see Fig).

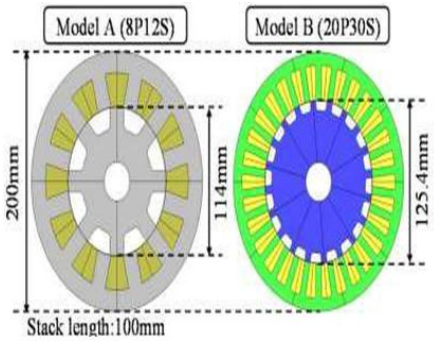

Fig.5. Motor structure of the proposed SRMs.

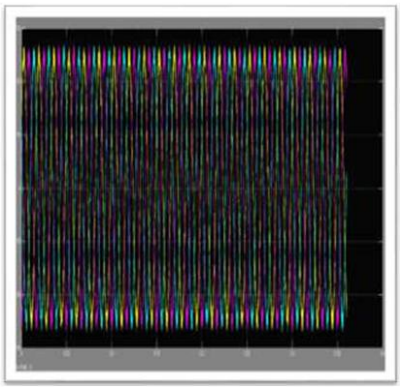

Fig.6. Current-Torque characteristic.

SIMULATION RESULTS

TABLE I
SPECIFICATION OF PROPOSED SRM

	Model A	Model B
Pole / Slot	8 / 12	20 / 30
Output power [kW]	85	34
Maximum speed [rpm]	50000	20000
Air gap length [mm]	0.5	0.5
Number of turns [turn/teeth]	5	5
Diameter of coil [mm]	6.0	4.0
Resistance [Ω/phase]	0.003	0.018
Core material	-	20H1200

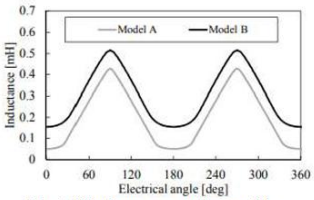

Fig. Self-inductance waveforms of the proposed SRMs.

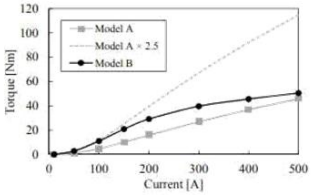

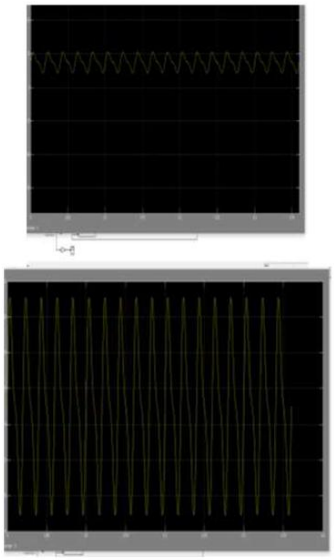

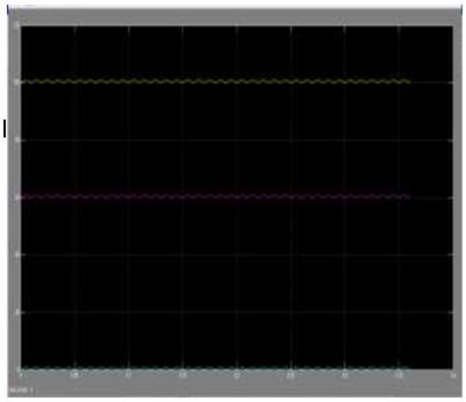

Fig.7. Self-inductance waveforms of the proposed SRMs.

CONCLUSION

In this study, the 20-pole 30-slot SRM that is driven at 20000 rpm and has the same electrical angular frequency as the 8-pole 12-slot SRM that is driven at 50000 rpm was constructed and assessed in order to apply vector control to the SRM in the high speed drive. Using a SiC inverter with a 200kHz switching frequency, the suggested motor met the required performance requirements for torque and output power in the vector control system. It was made clear through the experiment that the suggested SRM can be driven by vector control at the maximum rotational speed of 20,000 rpm. In other words, it means that the vector control can drive the 8-pole 12-slot SRM at a speed of 50,000 rpm. Finally, it was demonstrated that SRM vibration can be reduced in the high speed region by applying the vector control compared with that in the conventional single pulse drive.

REFERENCES

1. M. Besharati, J. Widmer, G. Atkinson, V.Pickert, Jamie Washington : “Super-high-speed switched reluctance motor for automotive traction”, IEEE Energy Conversion Congress and Exposition (ECCE), pp.5241-5248, September 2015.
2. Earl W. Fairall, Berker Bilgin, Ali Emadi :“State-of-the-ArtHigh-speed Switched Reluctance Machines”, IEEE International Electric Machines and Drives Conference (IEMDC), pp.1621-1627, May 2015.
3. M. N. Answar and Iqbal Husain, “Radial Force Calculation and Acoustic Noise Prediction in Switched Reluctance Machines”IEEE Transaction on Industry Application, Vol.36, No.6, pp.1589-1597, 2000.
4. Chenjie Lin and Babak Fahimi, Prediction of Radial Vibration in Switched Reluctance Machines”, IEEE Transaction on Energy Conversion, pp.250-258, Vol.29, No.1, 2014
5. H. Makino, T. Kosaka, Nobuyuki Matsui, “Digital PWMControl-Based Active Vibration Cancellation for Switched Reluctance Motors”, IEEE Transaction on Industry Application, Vol.51, No.6, pp.4521-4530, Nov 2015.
6. A. Tanabe, K. Akatsu, “Vibration reduction method in SRM with a smoothing voltage commutation by PWM”, 9th International Conference on Power Electronics and ECCE Asia (ICPE-ECCE Asia), June 2015.
7. K. M. Rahman, B. Fahimi, G. Suresh, A. V. Rajarathnam, and M. Ehsani, "Advantages of Switched Reluctance Motor Applications to EV and HEV: Design and Control Issues," IEEE Transactions on Industry Applications, vol. 36, No. 1, pp. 111-121, January/February 2000.
8. I. Husain and S. A. Hossain, "Modeling, Simulation, and Control of Switched Reluctance Motor Drives," IEEE Transactions on Industrial Electronics, vol. 52, No. 6, pp. 1625-1634, December 2005.
9. N. Nakao, K. Akatsu, “Vector control specialized for switched reluctance motor drives”, International Conference on Electrical Machines (ICEM), pp.943-949, September 2014.
10. N. Nakao, K. Akatsu, “Vector control for switched reluctance motor drives using an improved current controller”, IEEE Energy Conversion Congress and Exposition (ECCE), pp.1379-1386, Sept 2014.